

# Thermoluminescence glow curve analysis of Eu<sup>3+</sup> activated CaWO<sub>4</sub> phosphor

K. V. Dabre<sup>1</sup> and S. J. Dhoble<sup>2\*</sup>

<sup>1</sup>Department of Physics, Arts, Commerce & Science College, Koradi, Nagpur 441111, India

<sup>2</sup>Department of Physics, R.T.M. Nagpur University, Nagpur 440033, India

\*Corresponding author. E-mail: [sjdhoble@redffmail.com](mailto:sjdhoble@redffmail.com)

Received: 02 March 2013, Revised: 29 April 2013 and Accepted: 03 May 2013

## ABSTRACT

In this work we report the synthesis of CaWO<sub>4</sub> pure and doped by various concentration of Eu<sup>3+</sup> by solid state method. Crystallinity and formation of as-synthesized phosphors were confirmed by XRD technique. PL emission of the Eu<sup>3+</sup> activated as-synthesized phosphors shows the strong red emission at 619nm which corresponds to the characteristic transition <sup>5</sup>D<sub>0</sub> → <sup>7</sup>F<sub>2</sub> of Eu<sup>3+</sup> ion at excitation wavelength 273nm. TL glow curve of Eu<sup>3+</sup> activated CaWO<sub>4</sub> shows the two glow peaks was observed at 400K and 500K whereas undoped CaWO<sub>4</sub> shows only single peak observed at low temperature (354K). Doping effect on TL glow curve was discussed. Glow curve of Eu<sup>3+</sup> activated were fitted to five peaks which were analyzed and trap parameter were calculated by using Chens' method, and the dose response curve shows the phosphor is fairly sensitivity to lower dose also. Thus reported phosphor can be applicable in LED and environmental dosimetry. Copyright © 2013 VBRI press.

**Keywords:** Scheelite structured tungstate; thermoluminescence; glow curve analysis; photoluminescence; solid state diffusion; radiation dosimetry.



**K. V. Dabre** is Assistant Professor at Physics Department of Arts, Commerce and Science College, Koradi, Nagpur, India. His field of interest is exploring the new materials properties for the application in lamp industry and radiation dosimetry.



thermoluminescence, mechanoluminescence and lyoluminescence techniques. Dr. Dhoble published several research papers in International reviewed journals on solid-state lighting, LEDs, radiation dosimetry and laser materials. He is an executive member of Luminescence Society of India.

**S. J. Dhoble** obtained M.Sc. degree in Physics from Rani Durgavati University, Jabalpur, India in 1988. He obtained his Ph.D. degree in 1992 on Solid State Physics from Nagpur University, Nagpur. Dr. S. J. Dhoble is presently working as an Associate Professor in Department of Physics, R.T.M. Nagpur University, Nagpur, India. During his research carrier, he is involved in the synthesis and characterization of solid state lighting nanomaterials as well as development of radiation dosimetry phosphors using

## Introduction

Thermoluminescence (TL) dosimetry is one of the low cost and easy techniques to measure the radiation doses using TLD materials. Its simplicity of this technique had attracted much attention of researcher to make effort for seeking production of new high performance TLD material which leads researcher to take lots of efforts to study the properties and effects of various rare earths, transition metal ion as activator in the various host materials such as sulphates, Phosphates, Vanadate, borates, fluorides, oxides, tungstate for the betterment of such TLD materials [1-10]. Calcium tungstate has been extensively investigated because its wide applicability in various areas such as X-ray phosphors, scintillators, solid-state optoelectronic devices, lasers and optical fibers components and a distinguishing property of self activated blue emission related to tetrahedral WO<sub>4</sub><sup>2-</sup> groups [11-16]. Also CaWO<sub>4</sub> is a naturally occurring phosphor, which makes it more attractive to researcher among other alkaline earth metal tungstate with scheelite structure, again it owe good thermal and chemical stability due to tetrahedral symmetry of W<sup>6+</sup> coordinated with four Oxygen atoms. [14]. Tungstate has broad and intense emission bands due to charge transfer (CT) from oxygen to metal in the blue region. Doping of various rare earth ions are used to improve optical property of CaWO<sub>4</sub> [14-18] specially Eu<sup>3+</sup> has special importance because this rare earth doped in various host material has application in various fields were intelligent nanomaterials

require [19] and also the well established fact that there is efficient energy transfer  $\text{WO}_4^{2-}$  to  $\text{Eu}^{3+}$  [20]. Kang et al has studied the luminescent properties of  $\text{Eu}^{3+}$  in  $\text{MWO}_4$  ( $\text{M} = \text{Ca}, \text{Sr}, \text{Ba}$ ) matrix [21] which shows characteristic red emission of  $\text{Eu}^{3+}$  with long afterglow upon excitation of 254nm, and TL studies shows two peaks but the trap parameter calculation other than activation energy was not reported. Gayatri Sharma et al. have studied Effects of annealing on luminescence of  $\text{CaWO}_4:\text{Eu}^{3+}$  nanoparticles and its thermoluminescence study [22] but the TL analysis has not been made. The luminescence properties of  $\text{Eu}^{3+}$  doped  $\text{CaWO}_4$  has been widely made, but to the best of our knowledge TL studies of gamma irradiate  $\text{Eu}^{3+}$  doped  $\text{CaWO}_4$  is not studied, thus in this paper study the TL properties and defect produced in  $\text{CaWO}_4$  and  $\text{Eu}^{3+}$  doped  $\text{CaWO}_4$  is made. In the present work synthesis of calcium tungstate activated with  $\text{Eu}^{3+}$  rare earth ion. Photoluminescence (PL) and thermoluminescence properties of  $\text{CaWO}_4:\text{Eu}^{3+}$  synthesized by modified solid state synthesis are reported. Phase purity and formation of as-synthesized phosphors were confirmed by XRD technique. Molecular vibrations were analyzed by FTIR spectrum; whereas surface structure was analyzed by using SEM micrograph.

## Experimental

### Chemicals and apparatus

For synthesis of  $\text{CaWO}_4$  and  $\text{Eu}^{3+}$  doped  $\text{CaWO}_4$  phosphor by modified solid state method the starting chemicals were calcium carbonate ( $\text{CaCO}_3$ ) (Qualigens, AR 98%), Tungstic acid ( $\text{H}_2\text{WO}_4$ ) (Himedia, AR 99%), Europium Oxide ( $\text{Eu}_2\text{O}_3$ ) (Himedia, AR 99%) and sodium tungstate ( $\text{Na}_2\text{WO}_4$ ) (Himedia, AR 99%) used. Silica crucible, porcelain mortar pestle and high temperature muffle furnace were used to synthesize these phosphors and as synthesized material were characterized by X-ray diffractometer (XRD) (PANalytical X'Pert Pro) with  $\text{Cu K}\alpha$  radiation ( $\lambda = 0.15406 \text{ nm}$ ), scanning electron microscope (SEM) (JEOL, JSM-6380), Jobin Yvon Computerized Spectrofluorophotometer (JY3CS), a usual set up to record TL glow curve which consists of small kanthal plate (planchet) heated directly using temperature programme a photo multiplier tube (931B), a DC amplifier and a millivoltmeter strip chart recorder, FTIR (Shimadzu FTIR-8101A) with resolution of  $4.0 \text{ cm}^{-1}$  and a gamma source  $\text{Co}^{60}$  with the dose rate of  $0.463 \text{ kGy/h}$ .

### Synthesis and characterization

The stoichiometric amount of starting material was taken and crushed thoroughly using mortar pestle for 1 h. Then this crushed stoichiometric mixture of all reactants then transferred to porcelain crucible and heated for 6 h at about  $400^\circ \text{C}$  in air and after that allowed to cool slowly inside the furnace to room temperature. Same procedure of crushing 1 h and heating at different temperature was repeated first at  $800^\circ \text{C}$  for 24 h and then  $1000^\circ \text{C}$  for 4 h finally the highly sintered samples were soft milled to powder and used as is for further characterization. In order to dope  $\text{Eu}^{3+}$  in host lattice  $\text{Na}^+$  ion were incorporated for charge compensation and introduced through  $\text{Na}_2\text{WO}_4$ .

Resulting phosphors formation and phase identification of resulting final powder samples were tested by using a PANalytical X'Pert Pro X-ray diffractometer (XRD) with  $\text{Cu K}\alpha$  radiation ( $\lambda = 0.15406 \text{ nm}$ ) at operating voltage 40 kV, 30 mA for  $2\theta$  ranging from  $5^\circ$  to  $100^\circ$ . The surface morphology of resulting samples was analyzed by scanning electron microscope (SEM) (JEOL, JSM-6380) with cathode voltage 10 kV. Photoluminescence excitation and emission spectra of as synthesized samples were recorded on the JY3CS Jobin Yvon Computerized Spectrofluorophotometer. Pure and doped samples were exposed to different doses by gamma rays from  $\text{Co}^{60}$  source. TL glow curve were recorded with the heating rate  $2.5\text{K/min}$  from room temperature to  $300^\circ \text{C}$ . FTIR spectrum of pure (undoped) sample in the range  $400\text{--}4600 \text{ cm}^{-1}$  was recorded at room temperature with resolution of  $4.0 \text{ cm}^{-1}$ .

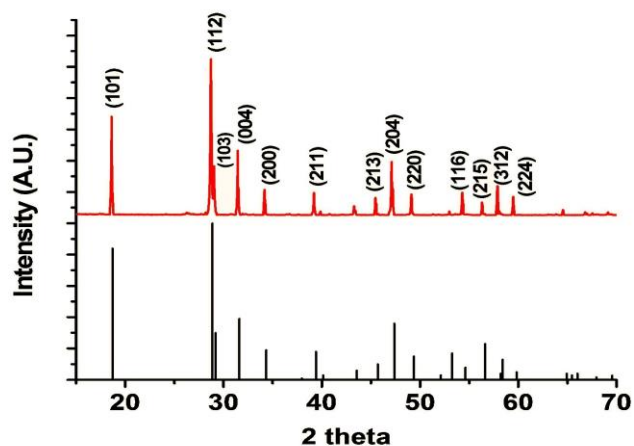


Fig. 1. X-ray powder diffraction pattern of  $\text{CaWO}_4$  phosphor.

## Results and discussion

Fig. 1 shows XRD pattern of resulting powder samples, and it is seen that all acquired diffraction peaks and calculated cell parameter are  $a = b = 5.26 \text{ \AA}$ ,  $c = 11.42 \text{ \AA}$  are in good agreement with standard data [23] of scheelite structure (see Fig. 2) of  $\text{CaWO}_4$  with tetragonal crystal system and  $I4_1/a$  space group. As-synthesized phosphor sample are said to be phase pure because no additional diffraction peaks are observed that could be attributed by the impurities.

Fig. 3 shows the morphology of resulting sample which reveals the formation of polycrystalline material with grain size shape distribution is irregular and average grain size is in sub-micrometer range due to agglomeration of smaller grains which forms due to thorough crushing and high temperature processing of the samples. This proves the solid state synthesis method is favorable for synthesis macro structured samples of reported phosphor.

Molecular stretching and bending properties were studied by using FTIR spectrum of as prepared  $\text{CaWO}_4:\text{Eu}^{3+}$  (0.1 mol %) phosphor sample is shown in Fig. 4. Owing to the  $S_4$  symmetry of  $\text{WO}_4^{2-}$  tetrahedrons in scheelite structured tungstate shows absorption bands in the region of  $400\text{--}1000 \text{ cm}^{-1}$  [11]. Fig. 4 shows the bands at  $438.7$ ,  $822.4$ ,  $1615.3$ , and  $3425.2 \text{ cm}^{-1}$  out of these bands the weak bands at  $3425.2$  and  $1615.3 \text{ cm}^{-1}$  are assigned to O–H stretching vibration and H–O–H bending vibration respectively [11,13]. These two bands are the characteristic

vibrations of water which corresponds to physically absorb on the sample surface. A strong absorption band at  $822.4\text{cm}^{-1}$  is related to O–W–O stretches of the  $\text{WO}_4^{2-}$  tetrahedron and that at  $438.7\text{cm}^{-1}$  has been attributed to the stretching vibration of W–O [13].

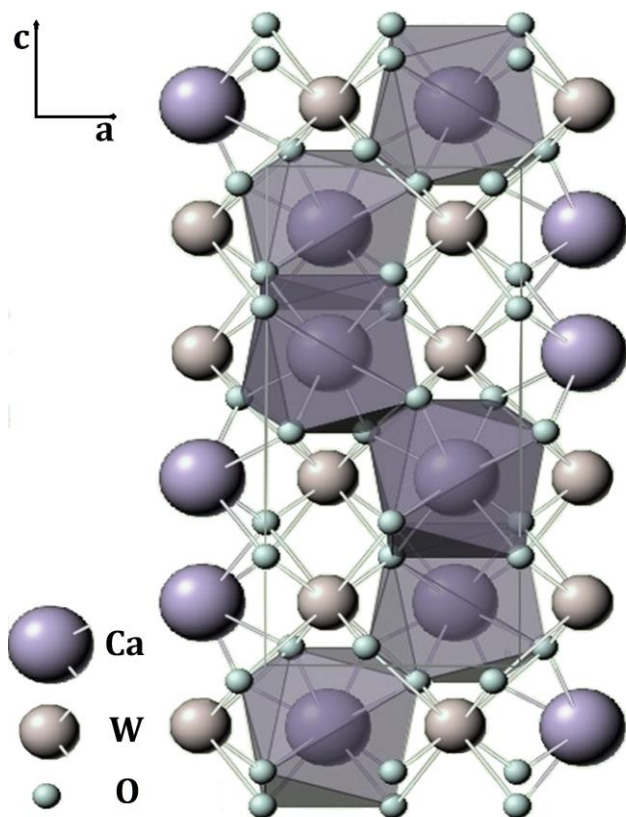


Fig. 2. Crystal structure of  $\text{CaWO}_4$  (Scheelite structured tungstate).

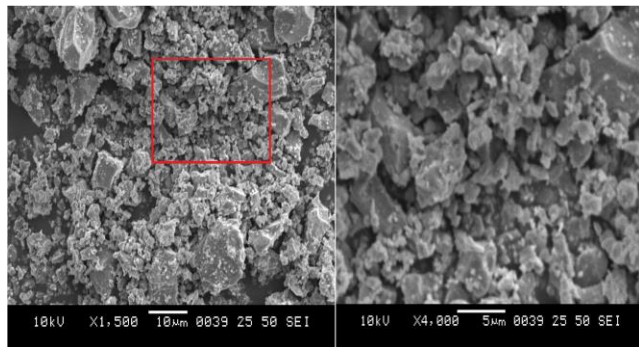


Fig. 3. SEM micrographic image of  $\text{CaWO}_4$  phosphor.

Photoluminescence excitation spectrum of  $\text{CaWO}_4:\text{Eu}^{3+}$  (0.1mol%) phosphor monitored at 619 nm is shown in Fig. 5 excitation spectrum shows broad band corresponds to ligands to metal charge transfer (LMCT)  $\text{WO}_4^{2-}$  group of  $\text{CaWO}_4$  [13]. It can be seen clearly that the excitation spectrum mainly consists of a broad band with maximum at 273nm which arise due to electric dipole (ED) allowed transitions ( $^1\text{A}_1 \rightarrow ^1\text{T}_1$ ,  $^1\text{T}_2$ ) of  $\text{WO}_4^{2-}$  group of host lattice ( $\text{CaWO}_4$ ) and strong lines at 398nm which is due to characteristic of f-f transition ( $^7\text{F}_0 \rightarrow ^5\text{L}_6$ ) of  $\text{Eu}^{3+}$  electrons in  $4f^6$  configuration [24,25].

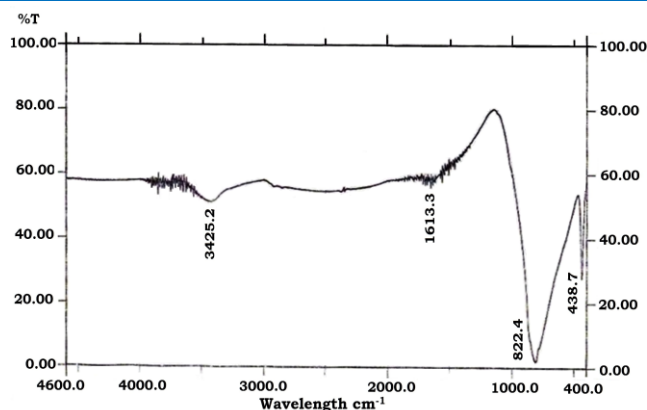


Fig. 4. FTIR spectra of  $\text{CaWO}_4$ .

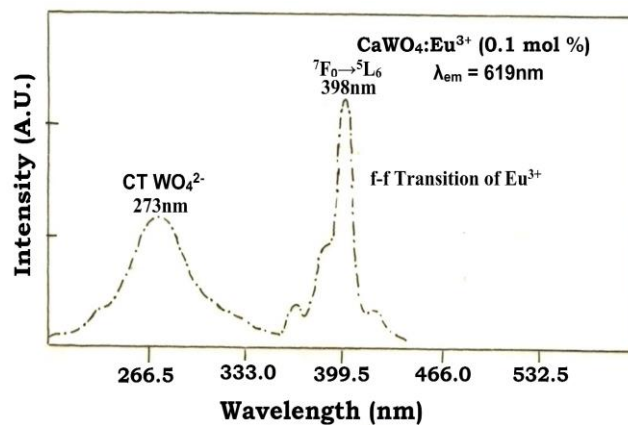


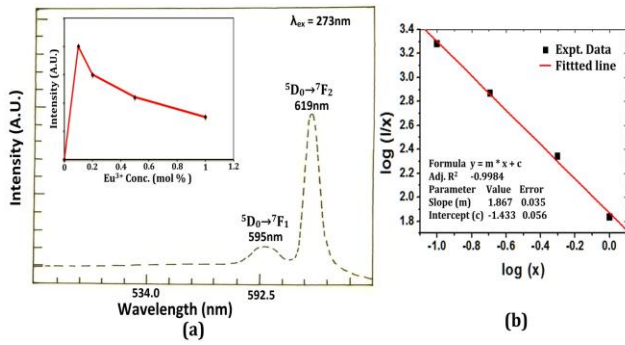
Fig. 5. PL Excitation spectra of  $\text{CaWO}_4:\text{Eu}^{3+}$  (0.1mol%) monitored at 619nm.

Fig. 6 shows the emission spectrum 0.1mol% of  $\text{Eu}^{3+}$  in  $\text{CaWO}_4$  lattice at excitation wavelength 273 nm and in inset shows the intensity ( $\lambda_{\text{em}} = 619\text{nm}$ ) variation with  $\text{Eu}^{3+}$  concentration in  $\text{CaWO}_4$  lattice. It is seen that the intensity is maximum for 0.1mol% and then decreases. The emission spectra show characteristic emission peaks at 595 and 619nm corresponding to magnetic dipole (MD) transition ( $^5\text{D}_0 \rightarrow ^7\text{F}_1$ ) and ED transition ( $^5\text{D}_0 \rightarrow ^7\text{F}_2$ ) respectively [13]. From the emission spectra of  $\text{Eu}^{3+}$  doped  $\text{CaWO}_4$  it can be easily predicted that  $\text{Eu}^{3+}$  occupies such a site in host matrix which lacks inversion symmetry, this is according to well known fact that ED transition is hypersensitive to site symmetry of  $\text{Eu}^{3+}$ , whereas MD transition is insensitive the ratio of red to orange emission is greater for non symmetric site (lacks inversion symmetry) [28].

It is obvious that to increase the emission intensity one has to increase activator concentration without getting quenching due to concentration which attributed to nonradiative energy transfer (ET) processes from  $\text{WO}_4^{2-}$  to  $\text{Eu}^{3+}$ . In order to find the optimum concentration of  $\text{Eu}^{3+}$  the intensity of ED transition ( $^5\text{D}_0 \rightarrow ^7\text{F}_2$ ) is observed for different concentration of  $\text{Eu}^{3+}$  and is shown in Fig. 6 (a) (Inset) the intensity of ED transition is maximum for 0.1 mol % concentration of  $\text{Eu}^{3+}$  in host matrix and beyond that it starts decrease because of dissipation of energy through nonradiative transitions which might be arises due to the defect structures caused by  $\text{Eu}^{3+}$  doping. Doping of  $\text{Eu}^{3+}$  causes to increase the defects in host lattice which is due to



the difference in ionic radius and charge compensation effects.



**Fig. 6.** PL Emission spectra of CaWO<sub>4</sub>:Eu<sup>3+</sup> (0.1 mol%) excited at 273 nm and in inset shows intensity variation of 619 nm peak with Eu<sup>3+</sup> concentration. Variation of 619 nm peak with Eu<sup>3+</sup> concentration. b) graph between log (I/x) and log (x) of Eu<sup>3+</sup>.

The critical distance  $R_c$  can be defined as the distance at which probability of ET is equally probable to radiative emission, in present case it is found to be 53.037 Å which can be calculated from the formula given by Blasse [29].

$$R_c = 2 \left( \frac{3V}{4\pi x_c N} \right)^{1/3}$$

where  $V$  is volume of unit cell  $x_c$  is concentration of Eu<sup>3+</sup> and  $N$  is number of host cation in unit cell. The interaction mechanism between Eu<sup>3+</sup> and WO<sub>4</sub><sup>2-</sup> can be evaluated by the expression given by Dexter [30].

$$\frac{I}{x} = k \left\{ 1 + \beta x^{\theta/3} \right\}^{-1}$$

where  $I$  is emission intensity and  $k$ ,  $\beta$  and  $\theta$  are the constant. When the value of  $\theta$  is 6, 8 and 10 it points the dipole-dipole, dipole-quadrupole and quadrupole-quadrupole interaction respectively and its value can be found out from the slope of log (I/x) Vs log (x) curve and is found to be  $\theta/3 = 1.867$  i.e  $\theta = 5.601 \approx 6$  which indicate the interaction between Eu<sup>3+</sup> and WO<sub>4</sub><sup>2-</sup> is dipole-dipole.

**Fig. 7** shows TL glow curve of as synthesized phosphors exposed to 6760 R gamma dose from Co<sup>60</sup> source and compared with CaSO<sub>4</sub>:Dy<sup>3+</sup> a standard thermoluminescent dosimeter (TLD) phosphor, and in inset **Fig. 7** shows variation of intensity of CaWO<sub>4</sub> with molar concentration of Eu<sup>3+</sup>. It is seen that only one glow curve of CaWO<sub>4</sub> at 358 K is obtained while CaWO<sub>4</sub>:Eu<sup>3+</sup> shows two glow curve one at 400 K and other one is at 500 K due to the luminescence defects centre's. It is also seen that TL emission intensity in doped (0.1 mol%) sample was thirteen times more than un-doped sample and fifty times less than CaSO<sub>4</sub>:Dy<sup>3+</sup> a standard thermoluminescent dosimetry (TLD) phosphor.

As early stated in the paper CaWO<sub>4</sub> crystallizes in a tetragonal scheelite structure with a space group of I41/a, in which Ca<sup>2+</sup> is surrounded by eight oxygen atoms and W<sup>6+</sup> coordinated with four oxygen atoms, during the

incorporation of Eu<sup>3+</sup> (ionic radius = 1.12 Å) in CaWO<sub>4</sub> host matrix Eu<sup>3+</sup> can acquire site either at Ca<sup>2+</sup> (ionic radius = 1.06 Å) or W<sup>6+</sup> (ionic radius = 0.63 Å) site. For the substitution of Eu<sup>3+</sup> at Ca<sup>2+</sup> leads to the defects complexes [2(Eu<sup>3+</sup>) + V<sub>Ca</sub>], similarly for W<sup>6+</sup> replacement the charge compensated as [2(Eu<sup>3+</sup>) + V<sub>W</sub> + 3V<sub>O</sub>] in order to compensate the charge, where V<sub>Ca</sub>, V<sub>W</sub> and V<sub>O</sub> are respectively vacancy of Ca, W and O atoms. [14] Later substitution is less favorable because of greater difference of ionic radii and oxidation states of ions but one it is substituted produces large number of defects which leads to broad glow curve.

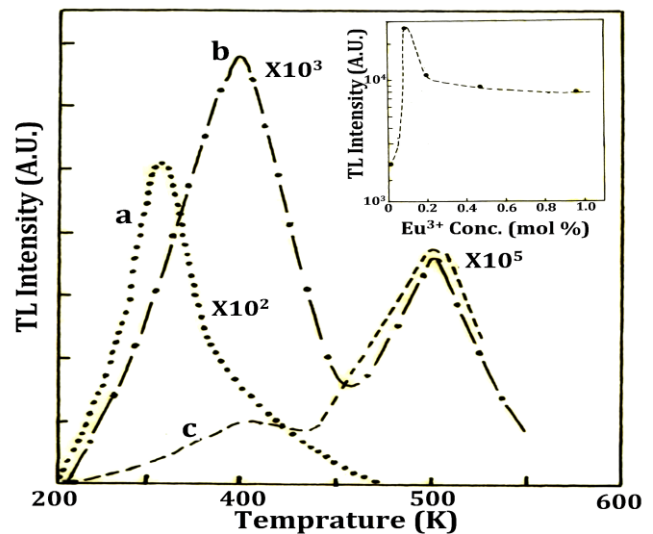


**Fig. 7.** TL Glow curve of a) CaWO<sub>4</sub>, b) CaWO<sub>4</sub>:Eu<sup>3+</sup> (0.1 mol%) and c) CaSO<sub>4</sub>:Dy<sup>3+</sup> and in Inset shows the variation of TL intensity with Eu<sup>3+</sup> concentration (in mol%).

**Table 1.** Trap parameter of CaWO<sub>4</sub> and CaWO<sub>4</sub>:Eu<sup>3+</sup> phosphors.

Sample (CaWO <sub>4</sub> :Eu <sup>3+</sup> )	T <sub>m</sub> (K)	μ <sub>g</sub>	γ	b	E <sub>avg</sub> (eV)	s (cm <sup>-1</sup> )
Peak 1	352	0.543	1.12	2	0.35	1.5 X 10 <sup>4</sup>
Peak 2	362	0.524	1.10	2	0.41	1.0 X 10 <sup>7</sup>
Peak 3	386	0.510	1.04	2	0.68	3.6 X 10 <sup>12</sup>
Peak 4	408	0.492	0.97	2	0.81	2.4 X 10 <sup>9</sup>
Peak 5	500	0.508	1.03	2	1.32	7.3 X 10 <sup>5</sup>

**Fig. 8** shows the experimental and deconvoluted TL glow curve of CaWO<sub>4</sub>:Eu<sup>3+</sup> (0.1 mol%). The kinetics and trap parameters of CaWO<sub>4</sub> and CaWO<sub>4</sub>:Eu<sup>3+</sup> (0.1 mol%) is calculated by using peak shape method [26] and are given in **Table 1**.

To calculate trap parameters by peak shape method then peak shape parameters  $\omega (= T_2 - T_1)$ ,  $\delta (= T_2 - T_M)$  and  $\tau (= T_M - T_1)$  are needed where  $T_1$  and  $T_2$  ( $T_1 < T_2$ ) are the temperature at half maximum intensity and  $T_M$  is temperature of maximum intensity. The order of kinetics can be predicted from shape of glow curve by using symmetry factor  $\mu_g$  stated by Chen can be given as

$$\mu_g = \frac{\delta}{\omega} = \frac{T_2 - T_M}{T_2 - T_1}$$

For first order kinetics  $\mu_g = 0.42$  and for second order kinetics  $\mu_g = 0.52$ . Another symmetry factor to identify the order of kinetics proposed by Balarin  $\gamma$  can be given as,

$$\gamma = \frac{\delta}{\tau} = \frac{T_2 - T_M}{T_M - T_1}$$

For first order kinetics  $\gamma$  ranges from 0.7 to 0.8 and for second order kinetics  $\gamma$  ranges from 1.05 to 1.20. From calculated values of  $\mu_g$  and  $\gamma$  it is seen that both peak corresponds to  $\text{CaWO}_4:\text{Eu}^{3+}$  (0.1mol%) is of second order kinetics. The activation energy (E) can be calculated by Chens [27] method and formula for activation energy can be given as,

$$E = c_\alpha \frac{kT_M^2}{\alpha} - b_\alpha (2kT_M)$$

where  $\alpha$  stands for  $\omega$ ,  $\tau$  and  $\delta$  respectively.  $c_\alpha$  and  $b_\alpha$  can be given as,

$$c_\tau = 1.51 + 3.0(\mu_g - 0.42) \text{ and}$$

$$b_\tau = 1.58 + 4.2(\mu_g - 0.42)$$

$$c_\delta = 0.976 + 7.3(\mu_g - 0.42) \text{ and } b_\delta = 0$$

$$c_\omega = 2.52 + 10.2(\mu_g - 0.42) \text{ and } b_\omega = 1$$

And the frequency factor's' can be calculated by the formula

$$s = \frac{\beta E}{kT_M^2} \frac{e^{E/kT_M}}{(1 + (b-1)2kT_M/E)}$$

where  $b$  is the order of kinetics and  $\beta$  is the heating rate.

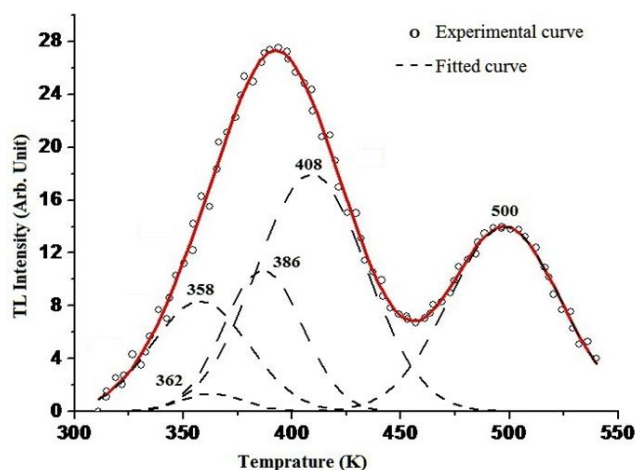


Fig. 8. Experimental and deconvoluted glow-curve of  $\text{CaWO}_4:\text{Eu}^{3+}$  (0.1mol%) irradiated by gamma from  $\text{Co}^{60}$  with a dose of 6760R and the heating rate was  $5^\circ\text{C}$ .

Fig. 9 Shows dose response curve of  $\text{CaWO}_4$  (351K),  $\text{CaWO}_4:\text{Eu}^{3+}$  (0.1m%) (394K) and  $\text{CaWO}_4:\text{Eu}^{3+}$  (0.1mol%)

(500K) from fig it is seen that range of linear response to absorbed dose in wide (i.e. 1R to 10kR) and after 10kR both phosphors shows saturation, it is also seen that  $\text{CaWO}_4$  has lowest sensitivity rather if it is doped with  $\text{Eu}^{3+}$  ion then the sensitivity enhances which shows the presence of  $\text{Eu}^{3+}$  ion makes  $\text{CaWO}_4$  easily susceptible to formation of defects on irradiation this may be due to the alliovalency of  $\text{Eu}^{3+}$  ion and difference of ionic radius.

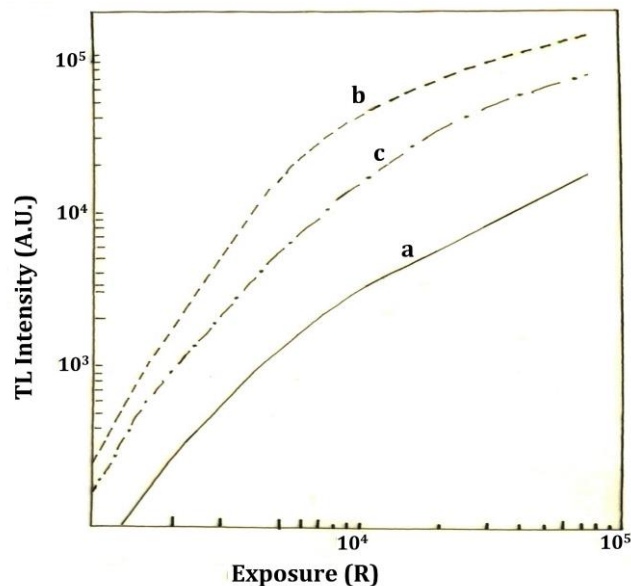


Fig. 9 TL gamma ray dose response curve of a)  $\text{CaWO}_4$  (351K glow peak) b)  $\text{CaWO}_4:\text{Eu}^{3+}$  (400K glow peak) and c)  $\text{CaWO}_4:\text{Eu}^{3+}$  (500K glow peak).

## Conclusion

In present work  $\text{CaWO}_4$  and  $\text{Eu}^{3+}$  doped  $\text{CaWO}_4$  phosphors were successfully synthesized by solid state reaction method and tested by X-ray diffraction pattern. SEM micrograph shows the formation of microcrystalline sample and FTIR spectrum shows the main transmittance peaks characteristic vibration of W-O bonds. The as synthesized  $\text{Eu}^{3+}$  doped  $\text{CaWO}_4$  phosphor material shows intense red emission at 619nm corresponding to characteristic transition  ${}^5\text{D}_0 \rightarrow {}^7\text{F}_2$  of  $\text{Eu}^{3+}$  ion at excitation wavelength 273nm. Analysis of TL glow curve shows the doping in the host matrix increases trap concentration also types of traps, also it enhances the TL sensitivity but little fall in linearity to dose response. Properties of the material show that it can be good candidate of TLD material.

## Reference

- McKeever S.W.S., *Thermoluminescence of Solids*, Cambridge University Press, 1983.  
DOI: [10.1063/1.2819986](https://doi.org/10.1063/1.2819986)
- Wani, J.A.; Atone, M.S.; Dhoble, N.S.; Dhoble, S.J., *Journal of Luminescence*, **2013**, *134*, 640.  
DOI: [10.1016/j.jlumin.2012.07.015](https://doi.org/10.1016/j.jlumin.2012.07.015)
- Bahl, S.; Lochab, S.P.; Pandey, A.; Aleynikov, V.E.; Molokanov, A.G.; Kumar, P., *Radiation Physics and Chemistry*, **2012**, *81*, 1683.  
DOI: [10.1016/j.radphyschem.2012.06.002](https://doi.org/10.1016/j.radphyschem.2012.06.002)
- Jiang, L.H.; Zhang, Y.L.; Li, C.Y.; Hao, J.Q.; Su, Q., *Applied Radiation and Isotopes*, **2010**, *68*, 196.  
DOI: [10.1016/j.apradiso.2009.10.001](https://doi.org/10.1016/j.apradiso.2009.10.001)
- Ignatovych, M.; Fasoli, M.; Kelemen, A., *Radiation Physics and Chemistry*, **2012**, *81*, 1528.  
DOI: [10.1016/j.radphyschem.2012.01.042](https://doi.org/10.1016/j.radphyschem.2012.01.042)

6. Wani, J.A.; Atone, M.S.; Dhoble, S. J., *Adv. Mat. Lett.* **2013**, *4*(5), 363.  
DOI: [10.5185/amlett.2012.10433](https://doi.org/10.5185/amlett.2012.10433)
7. Dhoble, S.J.; Shinde, K.N., *Adv. Mat. Lett.* **2011**, *2*(5), 349.  
DOI: [10.5185/amlett.2011.3072am2011](https://doi.org/10.5185/amlett.2011.3072am2011)
8. Singh, R.; Dhoble S. J., *Adv. Mat. Lett.* **2011**, *2*(5), 341.  
DOI: [10.5185/amlett.2011.3071am2011](https://doi.org/10.5185/amlett.2011.3071am2011)
9. Mahakhode, J.G.; Dhoble, S. J.; Moharil, S.V., *Adv. Mat. Lett.* **2011**, *2*(5), 331  
DOI: [10.5185/amlett.2011.3074am2011](https://doi.org/10.5185/amlett.2011.3074am2011)
10. Nimishe, P.; Dhoble, S.J., *Adv. Mat. Lett.* **2011**, *2*(5), 358.  
DOI: [10.5185/amlett.2011.3073am2011](https://doi.org/10.5185/amlett.2011.3073am2011)
11. Lei, F.; Yan, B., *J. Solid State Chem.*, **2008**, *181*, 855.  
DOI: [10.1016/j.jssc.2008.01.033](https://doi.org/10.1016/j.jssc.2008.01.033)
12. Lou, X.; Chen, D.; *Materials Letters*, **2008**, *62*, 1681.  
DOI: [10.1016/j.matlet.2007.09.066](https://doi.org/10.1016/j.matlet.2007.09.066)
13. Sharma, K.G.; Singh, N.R., *JOURNAL OF RARE EARTHS*, **2012**, *30*(4), 310.  
DOI: [10.1016/S1002-0721\(12\)60043-X](https://doi.org/10.1016/S1002-0721(12)60043-X)
14. Kang, F.; Hu, Y.; Wu, H.; Mu, Z.; Ju, G.; Fu, C.; Li, N., *Journal of Luminescence*, **2012**, *132*, 887.  
DOI: [10.1016/j.jlumin.2011.11.022](https://doi.org/10.1016/j.jlumin.2011.11.022)
15. Cornacchia, F.; Toncelli, A.; Tonelli, M.; Favilla, E.; Subbotin, K.A.; Smirnov, V.A.; Lis, D.A.; Zharikov, E.V., *J. Appl. Phys.*, **2007**, *101*, 123113-1.  
DOI: [10.1063/1.2749403](https://doi.org/10.1063/1.2749403)
16. Xiao, Q.; Zhou, Q.; Li, M., *Journal of Luminescence*, **2010**, *130*, 1092.  
DOI: [10.1016/j.jlumin.2010.02.001](https://doi.org/10.1016/j.jlumin.2010.02.001)
17. Nazarov, M.V.; Jeon, D.Y.; Kang, J.-H.; Popovici, E.J.; Muresan, L.-E.; Zamoryanskaya, M.V.; Tsukerblat, B.S., *Solid State Communications*, **2004**, *131*, 307.  
DOI: [10.1016/j.ssc.2004.05.025](https://doi.org/10.1016/j.ssc.2004.05.025)
18. Shi, S.; Gao, J.; Zhou, J., *Optical Materials*, **2008**, *30*, 1616.  
DOI: [10.1016/j.optmat.2007.10.007](https://doi.org/10.1016/j.optmat.2007.10.007)
19. Tiwari, A.; Mishra, A.K.; Kobayashi, H.; Turner, A. P.F.; *Intelligent Nanomaterials*, Wiley-Scrivener Publishing LLC, USA, **2012**.  
DOI: [10.1002/9781118311974](https://doi.org/10.1002/9781118311974).
20. Kang, F.; Hu, Y.; Chen, L.; Wang, X.; Wu, H., *Materials Science and Engineering B*, **2013**, *in press*.  
DOI: [10.1016/j.mseb.2013.01.021](https://doi.org/10.1016/j.mseb.2013.01.021)
21. Kang, F.; Hu, Y.; Chen, L.; Wang, X.; Wu, H.; Mu, Z., *Journal of Luminescence* **2013**, *135*, 113.  
DOI: [10.1016/j.jlumin.2012.10.041](https://doi.org/10.1016/j.jlumin.2012.10.041)
22. Sharma, K.G.; Singh, N.S.; Rangeela Devi, Y.; Singh, N. R.; Singh, D., *Journal of Alloys and Compounds* **2013**, *556*, 94.  
DOI: [10.1016/j.jallcom.2012.12.087](https://doi.org/10.1016/j.jallcom.2012.12.087)
23. Powder Diffraction File no.00-041-1431, JCPDS-ICSD.
24. Blasse, G.; Grabmaier, B.G., *Luminescent materials*, Springer-Verlag, **1994**.  
DOI: [10.1007/978-3-642-79017-1](https://doi.org/10.1007/978-3-642-79017-1)
25. Thongtem, T.; Phuruangrat, A.; Thongtem, S., *Applied Surface Science*, **2008**, *254*, 7581.  
DOI: [10.1016/j.apsusc.2008.01.092](https://doi.org/10.1016/j.apsusc.2008.01.092)
26. Pagonis, V.; Kitis, G.; Furetta, C., *Numerical and Practical Exercises in Thermoluminescence*, USA-Springer, **2006**.  
DOI: [10.1007/0-387-30090-2](https://doi.org/10.1007/0-387-30090-2)
27. Chen, R., *J. Electrochem. Soc.*, **1969**, *116* (9), 1254.  
DOI: [10.1149/1.2412291](https://doi.org/10.1149/1.2412291)
28. Yin, X.; Yao, J.; Wang, Y.; Zhao, C.; Huang, F., *Journal of Luminescence*, **2012**, *132*, 1701.  
DOI: [10.1016/j.jlumin.2012.02.006](https://doi.org/10.1016/j.jlumin.2012.02.006)
29. Blasse, G., *Phys. Status Solidi B*, **1973**, *55*, K131.  
DOI: [10.1002/pssb.2220550254](https://doi.org/10.1002/pssb.2220550254)
30. Dexter, D. L., *J. Chem. Phys.*, **1953**, *21*, 836.  
DOI: [10.1063/1.1699044](https://doi.org/10.1063/1.1699044)

## Advanced Materials Letters

Publish your article in this journal

**ADVANCED MATERIALS Letters** is an international journal published quarterly. The journal is intended to provide top-quality peer-reviewed research papers in the fascinating field of materials science particularly in the area of structure, synthesis and processing, characterization, advanced-state properties, and applications of materials. All articles are indexed on various databases including [DOAJ](https://doi.org/10.1002/DOAJ) and are available for download for free. The manuscript management system is completely electronic and has fast and fair peer-review process. The journal includes review articles, research articles, notes, letter to editor and short communications.

